ResearchGate

See discussions, stats, and author profiles for this publication at: https://www.researchgate.net/publication/372518225

Effect of gingival height of a titanium base on the biomechanical behavior of 2-piece custom implant abutments: A 3-dimensional nonlinear finite element study

Article *in* Journal of Prosthetic Dentistry · July 2023

DOI: 10.1016/j.prosdent.2023.06.031

CITATIONS
4

READS
322

7 authors, including:



Pongsakorn Poovarodom
Medical University of South Carolina
12 PUBLICATIONS **62** CITATIONS
SEE PROFILE



Chaiy Rungsiyakull
Chiang Mai University
46 PUBLICATIONS **624** CITATIONS
SEE PROFILE



Jarupol Suriyawanakul
Khon Kaen University
19 PUBLICATIONS **31** CITATIONS
SEE PROFILE



Qing Li
The University of Sydney
524 PUBLICATIONS **23,979** CITATIONS
SEE PROFILE

All content following this page was uploaded by Pimduen Rungsiyakull on 22 July 2023.

The user has requested enhancement of the downloaded file.

THE JOURNAL OF PROSTHETIC DENTISTRY

RESEARCH AND EDUCATION

Effect of gingival height of a titanium base on the biomechanical behavior of 2-piece custom implant abutments: A 3-dimensional nonlinear finite element study

Pongsakorn Poovarodom, DDS, MSc,[a] Chaiy Rungsiyakull, BEng, MEng, PhD,[b] Jarupol Suriyawanakul, BEng, MEng, PhD,[c] Qing Li, BE, ME, PhD,[d] Keiichi Sasaki, DDS, PhD,[e,f] Nobuhiro Yoda, DDS, PhD,[g] and Pimduen Rungsiyakull, DDS, MDSc, PhD, FRCDS[h]

ABSTRACT

Statement of problem. Titanium base (TiBase) abutments to restore an implant-supported single crown are available in different gingival heights, but information on the biomechanical effects of the gingival heights is lacking.

Purpose. The purpose of this nonlinear finite element analysis study was to evaluate the effects of TiBase gingival heights on the biomechanical behavior of custom zirconia (CustomZir) abutments and TiBase, including von Mises stress and maximum and minimum principal stress.

Material and methods. TiBases with different gingival heights (0.5 mm, 1 mm, 1.5 mm, and 2 mm) with internal hexagon Morse taper connections were simulated in 3-dimensional models. The simulations (ANSYS Workbench 2020; ANSYS Inc) included the OsseoSpeed EV implant (Ø5.4 mm) (AstraTech; Dentsply Sirona), restoration, and surrounding bone in the mandibular first molar region. An occlusal force of 200 N was applied with a 2-mm horizontal offset toward the buccal side and a 30-degree inclination from the vertical axis.

Results. High-stress concentration was observed in the uppermost internal connection area on the buccal side and the antirotational part of the titanium abutment on the lingual side in all models. CustomZir abutments with a shorter gingival height exhibited larger concentrated areas of volume average stress von Mises stress and higher magnitude of maximum and minimum principal stress compared with a taller gingival height.

Conclusions. A TiBase abutment with a taller gingival height reduced the fracture risk of a CustomZir abutment without increasing any mechanical risk. (J Prosthet Dent 2023;xxx:1.e1-e9)

With the emergence of digital dentistry, dental laboratory technicians can generate custom abutments by using computer-aided design and computer-aided manufacturing (CAD-CAM) technologies.[1,2] Abutments can be fabricated from different materials, including titanium and zirconia ceramic.[2] The zirconia abutment was developed as an alternative to the titanium abutment to overcome the gray color at the free gingival margin[3,4] and because of its exceptional mechanical properties compared with other ceramics.[4,5] In vitro and in vivo studies have determined the excellent biocompatibility of zirconia, enabling effective fibroblast and epithelial cell adhesion to its surface,[6–11] but with lower bacterial adherence than titanium[12–14] because zirconia has low surface free energy.[15,16] However, zirconia abutments have disadvantages, including wear at the implant-abutment contact area,[17] resulting in implant-abutment

The authors declare the following financial interests/personal relationships, which may be considered potential competing interests.
[a]PhD candidate, Department of Prosthodontics, Faculty of Dentistry, Chiang Mai University, Chiang Mai, Thailand.
[b]Assistant Professor, Department of Mechanical Engineering, Faculty of Engineering, Chiang Mai University, Chiang Mai, Thailand.
[c]Assistant Professor, Department of Mechanical Engineering, Faculty of Engineering, Khon Kaen University, Khon Kaen, Thailand.
[d]Professor, School of Aerospace, Mechanical and Mechatronic Engineering, Faculty of Engineering, The University of Sydney, Sydney, NSW, Australia.
[e]President, Miyagi University, Taiwa, Miyagi, Japan.
[f]Executive Adviser, Tohoku University, Sendai, Miyagi, Japan.
[g]Senior Assistant Professor, Division of Advanced Prosthetic Dentistry, Tohoku University Graduate School of Dentistry, Sendai, Miyagi, Japan.
[h]Associate Professor, Department of Prosthodontics, Faculty of Dentistry, Chiang Mai University, Chiang Mai, Thailand

Clinical Implications

Selecting a titanium base abutment with a short gingival height presents a fracture risk for custom zirconia abutments because of the high-stress concentration in the cervical area.

micromovement[18] and possible discoloration of the gingiva.[19] Consequently, a 2-piece zirconia abutment or hybrid abutment was invented to overcome wear at the implant-abutment interface. This titanium base (TiBase) abutment consists of a titanium component that contacts the dental implant and a transmucosal zirconia component, the custom zirconia (CustomZir) abutment.[20,21]

TiBase abutments are available in designs with gingival heights ranging from 0.5 to 2 mm, depending on the dental implant system.[22–24] A correlation has been reported between abutments with a short gingival height and marginal bone loss (MBL),[14,25–28] possibly because the wider abutment shape on the TiBase compresses the peri-implant mucosa and affects the re-establishment of the biological width.[27,28] The gingival height has been reported to have a considerably greater impact on MBL than platform switching or abutment connection type.[26] Theoretically, using a TiBase with a taller gingival height to connect the crown or CustomZir to the implant would allow for improved soft-tissue adaptation, positioning the junction between the crown and the abutment supragingivally and reducing bacteria-induced inflammation and minimizing bone resorption.[29] In terms of mechanical strength, the integration of a TiBase may benefit the stability of hybrid zirconia abutments by increasing structural resistance to occlusal force[30] and increasing the fracture resistance of the prosthesis.[21,31] As a result, it has been theorized that the TiBase may assist in reducing stress in the cervical region of the emergence profile.[32]

The optimal gingival height of a TiBase abutment that enhances abutment connection stability and implant connection stability remains unknown. The finite element (FE) method has been used to investigate relationships between implant abutment design, stress distribution, deformation, and confounding variables.[33–37] FE simulations give critical information on the actual biomechanical properties of the implant assembly, such as stress, strain energy, and bone density at any spatial and temporal location within the assembly.[33–36]

The purpose of this research was to determine the effect of the different gingival heights of TiBases on stresses occurring in the implant complex for a delayed-loading implant in the mandibular first molar region. Therefore, a relationship was established between the gingival height of the TiBase abutment and its associated mechanical parameters, particularly von Mises stress and maximum and minimum principal stress, through the use of nonlinear finite element analysis (FEA). The null hypothesis was that the different gingival heights of TiBases would not result in different stress values in the implant components or in the peri-implant bone.

MATERIAL AND METHODS

Four 3-dimensional (3D) models of the TiBase abutment with different gingival heights (0.5 mm, 1.0 mm, 1.5 mm, and 2.0 mm) were constructed (Figs. 1, 2). Each model consisted of the virtual models of a Ø5.4 × 11-mm implant (OsseoSpeed EV, AstraTech; Dentsply Sirona) with a TiBase abutment (TitaniumBase AT EV 5.4 GH1 L, AstraTech; Dentsply Sirona), a Ø5.4 × 5-mm retention post, and 4 different gingival heights. The TiBase abutment was secured to the implant using a Ø2 × 7.6-mm abutment screw (Screw AT EV 5.4, AstraTech; Dentsply Sirona). The custom abutment on a TiBase and the zirconia crown was fabricated (10 mm buccolingual, 12 mm mesiodistal, and with 8-mm interocclusal space). All components were designed and remodeled with a software program (SolidWorks 2017; SolidWorks Corp). A mandibular section of the bone in the molar area was constructed by using the images from a cone beam computed tomography (CBCT) scanner (Varaview X800; MORITA), in which the CBCT images were processed in a 3D computer graphics and CAD application software program (Rhinoceros 3D; Robert McNeel and Associates). The bone sections were modeled with 2 segments: the outer shell, with an average thickness of approximately 2 mm representing the cortical bone, and an inner continuum core representing the cancellous bone, which was assumed to be perfectly bonded with the cortical layer.[38] The contact boundary condition of the implant-abutment and abutment-screw contact was assigned as a frictional contact with a friction coefficient of 0.4.[39] Furthermore, the contact function of the bolt thread had been assigned to the interface between the abutment screw thread surface and the female screw component inside the implant. The parameters encompassed a single right-handed thread type with a mean pitch diameter of 1.88 mm, a pitch distance of 0.4 mm, and a thread angle of 37.1 degrees.

The bolt was tightened to 25 Ncm[40] as defined by the Bolt Pretension function in the ANSYS software. In contrast, a bond contact was applied to the contact between the bone implant and the abutment crown. The interface of the TiBase abutment, zirconia custom abutment, and zirconia crown was completely seated without any gap, and the cement layer was excluded.[41–43] The mechanical properties of an implant, abutment, screw, and crown are listed in Table 1. All materials were assumed to be isotropic, homogeneous,

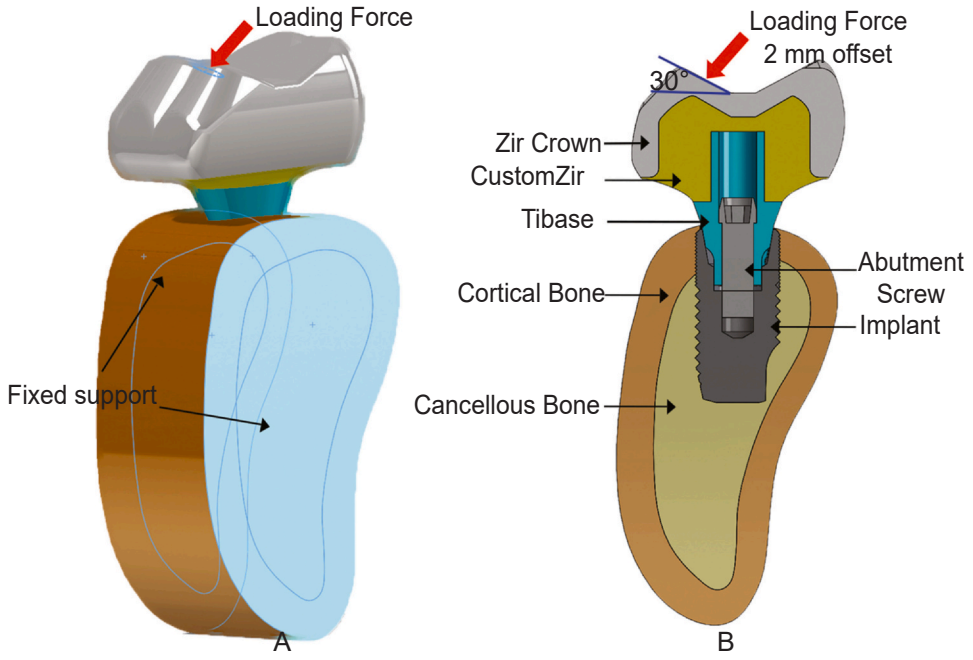


Figure 1. A, Full isotropic view of finite element model with loading and boundary condition. B, Buccolingual cross-section view of model with components labeled.

and linearly elastic.[38,44,45] All the associated hard tissues were also assumed to be linearly elastic and isotropic to simplify analysis.[46]

A mechanical load of 200 N[47] was applied on the occlusal surface with a 2-mm horizontal offset toward the buccal side and a 30-degree inclination from the vertical axis. The fixed support boundary conditions were assigned at the mesial and distal sectional surfaces of the bone model to represent surrounding bone support. The FE mesh densities of all parts in this study were confirmed to have adequate accuracy and computing efficiency by a convergence study; the result showed that the suitable element size was 0.4 mm. A contact size of 0.1 mm was assigned at the abutment screw-implant contact surface. The 3D 10-node tetrahedral solid element (SOLID187) was adopted with an average of 900 000 elements and 600 000 nodes for all 4 FE models. The FEA was performed with a simulation software program (ANSYS Workbench 2020; ANSYS Inc) on a workstation computer (Intel(R) Xeon(R) Silver 4114 CPU 20 Core 2.20 GHz; Intel Corp).

The effects of varying gingival height of the TiBase on implant components were explored in the context of 6 parameters: von Mises stress distribution, volume average von Mises stress, percentage difference of maximum von Mises stress in each component between different gingival height models, maximum von Mises stress, the stress distribution and highest (in magnitude) of maximum and minimum principal stress. To mitigate the impact of peak stress bias caused by model artifacts,

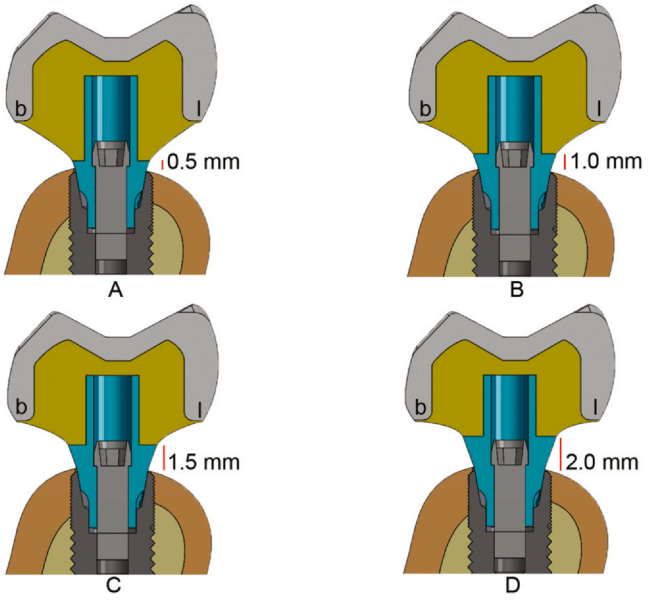


Figure 2. Buccolingual cross-section views of all testing models. A, GH0.5. B, GH1. C, GH1.5, and D, GH2. b, buccal side; l, lingual side.

Table 1. Material properties of implant, abutment, crown, and bone

Materials	Properties	
	Young Modulus (GPa)	Poisson Ratio
Titanium Commercially Pure grade IV	110	0.3
Zirconia (ZrO_2)	200	0.35
Cortical bone	11.67	0.3
Cancellous bone	1.872	0.3

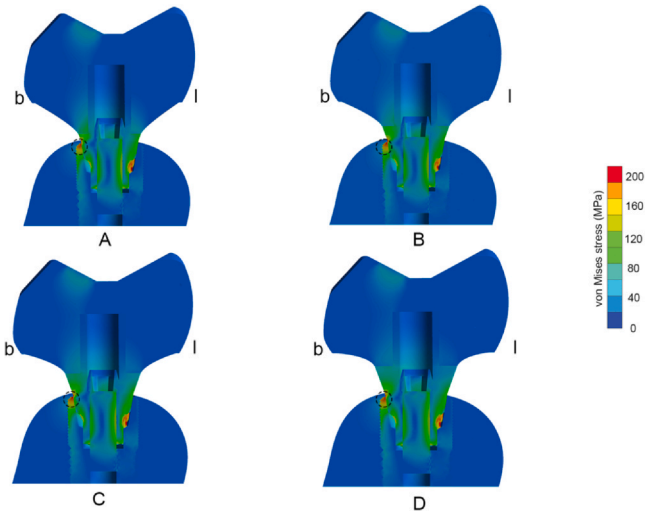


Figure 3. Buccolingual cross-sectional view of all tested models of von Mises stress distribution in A, GH0.5. B, GH1. C, GH1.5. D, GH2. *Black circle* represents location of maximum von Mises stress. b, buccal side; l, lingual side.

the concept of volume-averaged von Mises stress was introduced. This parameter combines and averages the stress values across a specific region of each element, considering both the volume of each element and the total volume of all elements. The calculation of this parameter is represented by Equation 1. Equation 2 was used to calculate the percentage difference. The volume average von Mises stress was used to evaluate the average von Mises stress value for each element in all 4 abutments. This allowed for a meaningful comparison among the different models, enabling the identification of the component that experienced the highest overall stress in each model.[48–51]

$$\text{Volume average von Mises stress} = \frac{\sum (\text{stress} \times \text{volume by element})}{\sum \text{volume}} \quad (1)$$

$$\text{Percentage difference} = \frac{(\text{high value} - \text{low value}) \times 100}{\text{low value}}. \quad (2)$$

RESULTS

The von Mises stress was first evaluated in terms of distribution pattern and maximum stress value. The results revealed that the characteristics of stress distribution in all models were similar (Fig. 3). The majority of stress concentration was found at the antirotational part of the TiBase on the lingual side, microthread of the implant on the buccal side, abutment screw, and abutment connection. The highest stress location was detected at the Morse taper internal connection in the implant platform area of the buccal side. In the abutment screw, the stress concentration was higher on the lingual than on the buccal side, whereas in TiBase, the stress concentration was found on both sides.

Figure 4 presents the volume average von Mises stress values. The results indicated that TiBase exhibited the highest volume average stress value, which was 5 times higher than the implant within the range of 49 to

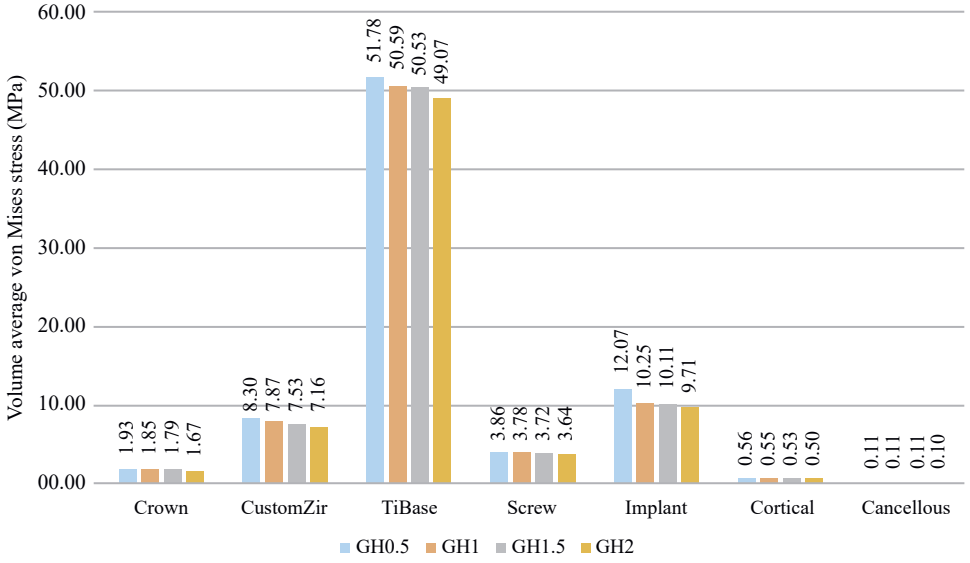


Figure 4. Volume average von Mises stress of crown, custom zirconia (CustomZir) abutment, titanium base (TiBase) abutment, abutment screw (Screw), implant, cortical bone, and cancellous bone in each model.

Table 2. Percentage difference of volume average von Mises stress of components in each model

	Model Difference (%)			
Component	**GH0.5**	**GH1**	**GH1.5**	**GH2**
Crown	15.3	10.6	7.4	0
CustomZir	16.0	9.9	5.1	0
TiBase	5.5	2.9	2.9	0
Screw	5.9	3.7	1.9	0
Implant	24.3	5.5	4.1	0
Cortical	12.3	10	7	0
Cancellous	18.2	14.5	10.4	0

CustomZir, custom zirconia; TiBase, titanium base.

51.7 MPa. In contrast, the cancellous bone appeared to have the lowest volume average stress, approximately 0.1 MPa. As the gingival height increased, there was a corresponding decrease in the volume average stress value for all components.

The percentage difference served as a measure of the relative value of the volume average von Mises stress for the same components across all models, as shown in Table 2. A consistent pattern was observed in all components, where the GH0.5 model exhibited the highest percentage difference values. Particularly in the case of implant components, the difference was most pronounced, with a significant percentage difference of 24.3% compared with GH2. However, TiBase demonstrated the lowest percentage difference, with only a 5.5% deviation when compared with GH2.

The maximum von Mises stress in implants and components is shown in Figure 5, where implants and TiBase generally exhibit the highest von Mises stress in the range of 287 to 302 MPa across the models. The maximum von Mises stress in the crown, abutment screw, and implant appeared to be comparable among testing models. However, the highest von Mises stress in TiBase and CustomZir was seen differently, as the greater the gingival height of TiBase, the lower the measured maximum stress value in TiBase and CustomZir. CustomZir demonstrated that the highest stress was recorded at GH0.5 with a value of 81.9 MPa, while GH2 had the lowest stress level of 40.8 MPa. TiBase demonstrated that the highest stress was recorded at GH0.5 with a value of 299.1 MPa, while GH2 had the lowest stress level of 279.6 MPa.

The maximum and minimum principal stresses were interpreted jointly with regard to the distribution pattern and maximum stress value. In the CustomZir component, most of the principal stress concentration was localized in the cervical region, as depicted in Figure 6. At the lingual of the TiBase-CustomZir interface, the peak (in magnitude) maximum principal stress values and high-stress zone (red color in the upper row) were detected. However, the peak (in magnitude) minimum principal stress (blue color in the bottom row) concentrations were detected on the buccal side of CustomZir. Model GH0.5 (Fig. 6A, E) revealed the largest area of high (in magnitude) maximum principal (red color in the upper row) and minimum principal stress (blue color in the bottom row). The peak (in magnitude) maximum and minimum principal stresses of CustomZir on every model are presented in Table 3. Model GH0.5 has the greatest values (in magnitude) for both stresses, 72 MPa and −102.3 MPa. Comparatively, the highest stress (in magnitude) of GH2 was 39.8 MPa and −51.7 MPa. Notably, as the gingival height ratio of TiBase grew, the area of high-stress concentration and peak stress value dropped, especially on GH2.

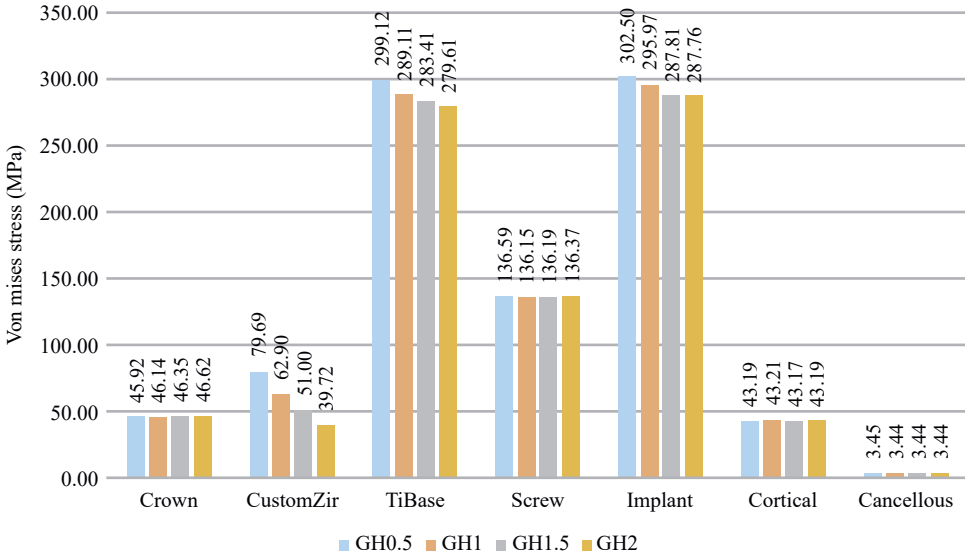


Figure 5. Maximum von Mises stress of crown, custom zirconia (CustomZir) abutment, titanium base (TiBase) abutment, abutment screw (Screw), implant, cortical bone, and cancellous bone in each model.

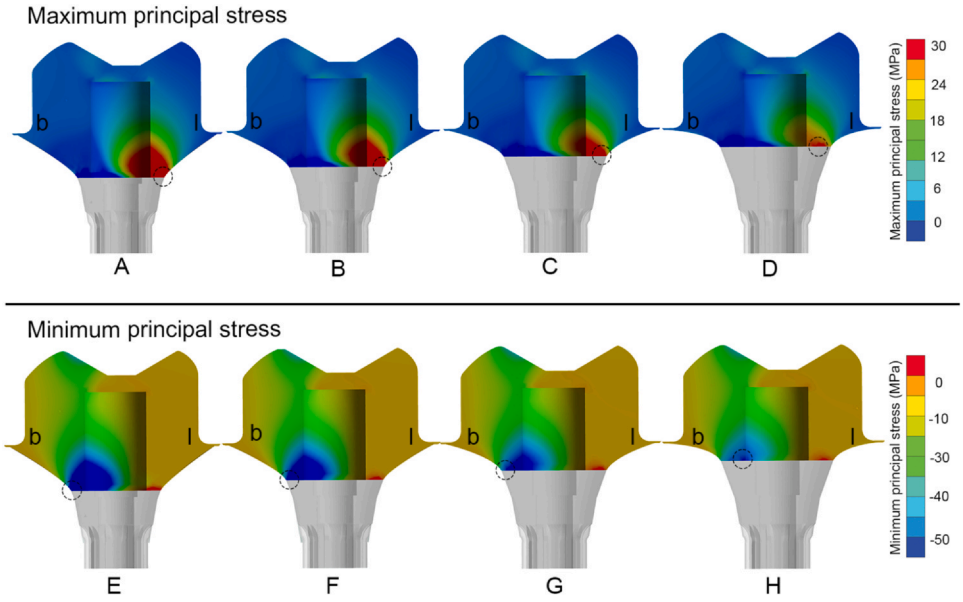


Figure 6. Buccolingual cross-sectional view of all custom zirconia (CustomZir) abutment models. (b) buccal side, (l) lingual side, of maximum (upper row) and minimum principal stress (lower row) distribution in: (A, E) GH0.5. (B, F) GH1. (C, G) GH1.5. (D, H) GH2. *Black circle* represents location of peak (in magnitude) maximum and minimum principal stress.

Table 3. Peak (in magnitude) of maximum and minimum principal stress of CustomZir and TiBase in each model

Component	Peak Stress (MPa)	Model			
		GH0.5	GH1	GH1.5	GH2
CustomZir	Maximum principal	72	58.3	44.3	39.8
	Minimum principal	−102.3	−83.5	−65.7	−51.6
TiBase	Maximum principal	337.3	322.5	321.3	317.9
	Minimum principal	−319.3	−318.4	−316.8	−304.4

CustomZir, custom zirconia abutment; TiBase, titanium base.

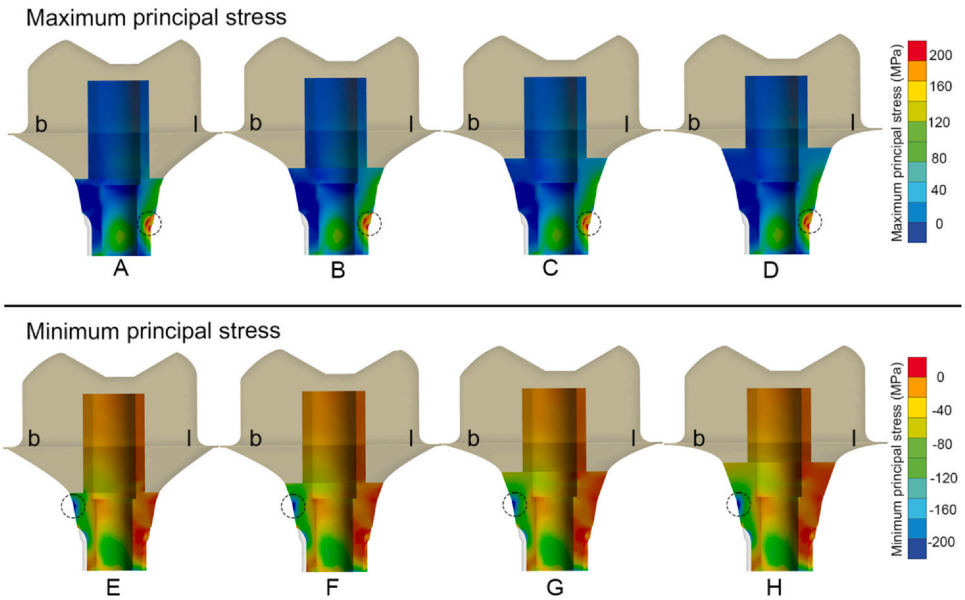


Figure 7. Buccolingual cross-sectional view of all titanium base (TiBase) models. (b) buccal side, (l) lingual side, of maximum (upper row) and minimum principal stress (lower row) distribution in: (A, E) GH0.5, (B, F) GH1, (C, G) GH1.5, and (D, H) GH2. *Black circle* represents location of peak (in magnitude) maximum and minimum principal stress.

In the TiBase component, much of the high-stress concentration was located in the antirotational part region and conical connection surface of TiBase, as depicted in Figure 7. The peak (in magnitude) maximum principal stress values and a zone of high-stress concentration were observed (red color in the upper row) at the lingual antirotational interface, whereas the concentration of the peak (in magnitude) minimum principal stress was seen (blue color in the lower row) at the conical connection on the buccal interface. Evidently, as the gingival height ratio of TiBase increased, the TiBase-CustomZir interface migrated away from the region of high-stress concentration, particularly on GH2. The peak (in magnitude) maximum and minimum principal stresses of TiBase on every model are illustrated in Table 3. GH0.5 exhibited the highest maximum principal stress of 337.3 MPa and the peak (in magnitude) minimum principal stress of −319.3 MPa, whereas GH2 exhibited the lowest levels of both stresses at 317.9 MPa and −304.4 MPa.

DISCUSSION

The current investigation demonstrated that the gingival height of the TiBase has an impact on the mechanical response, specifically in terms of stress concentration, within the abutment connection of a 2-piece CustomZir abutment complex. This finding highlights the significance of TiBase as an important component in the restoration of implant-supported single crowns. Thus, the null hypothesis that different gingival heights would not result in different stress values in implant components and peri-implant bones was rejected.

The volume average von Mises stress analysis revealed that TiBase experienced higher stress levels in each component compared with the other elements. This finding implies that TiBase plays an essential role in receiving and transmitting the occlusal load to the implant, abutment screw, and peri-implant bone.[52] The finding was consistent with that of a previous study that concluded TiBase contributes to improved stress distribution at the implant in zirconia abutments with a TiBase by absorbing stress internally.[48] Notably, as the gingival height increased, a simultaneous decrease in the volume average stress value was seen across all components. Particularly in the case of the implant, there was a notable reduction of 24.3% when comparing GH0.5 with GH2. As a result, selecting a TiBase with increased gingival height can help reduce the chance of implant damage.

In the current study, the gingival height of the TiBase had a considerable impact on both CustomZir-related stresses and its own stress levels. The results indicated that a TiBase with an increased gingival height may reduce the maximum and high-stress concentration areas of von Mises stress and the maximum and minimum principal stress in CustomZir (Figs. 3, 6). This reduction may have resulted from the titanium-to-zirconia ratio in the 2-piece zirconia custom abutment. Consequently, sufficient core thickness may be important.[53] As the gingival height of TiBase increased, the thicker CustomZir connection with TiBase was observed, resulting in the increasing rigidity of this abutment complex. The rigidity of the core material plays an essential role, as a stiffer core can better withstand flexure caused by loading. Furthermore, as the gingival height of the TiBase increased, the TiBase-CustomZir interface shifted away from areas of intense stress because the area of high-stress concentration was positioned near the implant abutment junction. This junction is part of the implant-abutment complex that experiences the most movement when subjected to occlusal load, which can cause significant stress concentration at the TiBase-CustomZir interface, particularly with a short gingival height. Therefore, increasing the gingival height should reduce the risk of clinical CustomZir fracture.

Many FEA studies have assumed all model components to be perfectly bonded at all interfaces (linear FEA), and high-stress concentration had been observed at the first thread of implant or loading area.[33–36] However, in the present study, the majority of the high von Mises stress concentrations were found at the antirotational part and Morse taper connection of the abutment, the abutment screw shank, and the first thread of the implant on the buccal side (Fig. 3). This result differed from linear FEA, and the results could be important, as these high-stress concentration regions can predict the chances of mechanical complications, which coincide with common implant complications, including screw loosening, abutment fracture, and MBL.[54] In addition, a region containing high (in magnitude) maximum principal stress was observed in CustomZir at the lingual contact area between the TiBase and CustomZir (Fig. 6), an area reported to have the highest stress concentration as a result of bending effects, in which the customize zirconia abutment fractured, as is typically observed in laboratory tests.[55–57] Hence, nonlinear FEA could provide more information with greater clinical relevance than linear FEA.

According to the findings, TiBase with an increased gingival height could reduce the risk of CustomZir abutment fracture without increasing any mechanical risk. Furthermore, increased gingival height has been reported to be more advantageous to biological integrity by minimizing MBL and maintaining biological width.[14,25–28] However, further optimization research is required to identify the optimal TiBase gingival height and shape.

Limitations of this study include the in silico analysis, and that validation is required with clinical investigation. In silico analysis differs from the clinical setting and the actual properties of materials, as well as the precise shape of the implant and its components, particularly the TiBase abutment. The findings obtained could be applied to compare implant designs that incorporate an internal hexagon and a Morse taper abutment connection, as different abutment connections affect mechanical behavior. Current research may enhance the understanding of biomechanical factors in choosing the optimal TiBase abutment and in forecasting complications.

CONCLUSIONS

Based on the findings of this 3D nonlinear FE study, the following conclusions were drawn:

1. The gingival height of the TiBase has a direct effect on the shape and stress concentration area of a CustomZir abutment.
2. A wider zirconia custom abutment led to a lower stress concentration pattern at the TiBase-CustomZir connection.
3. When selecting the TiBase, it is advisable to choose one of increased gingival height, as it demonstrates better mechanical behavior compared with a shorter gingival height.

REFERENCES

1. Kapos T, Evans C. CAD/CAM technology for implant abutments, crowns, and superstructures. *Int J Oral Maxillofac Implant*. 2014;29:117–136.
2. Ferrari M, Vichi A, Zarone F. Zirconia abutments and restorations: From laboratory to clinical investigations. *Dent Mater*. 2015;31:63–76.
3. Farrag KM, Khamis MM. Effect of anodized titanium abutment collars on peri-implant soft tissue: A split-mouth clinical study. *J Prosthet Dent*. 2021;28:59–67.
4. Holst S, Blatz MB, Hegenbarth E, Wichmann M, Eitner S. Prosthodontic considerations for predictable single-implant esthetics in the anterior maxilla. *J Oral Maxillofac Surg*. 2005;63:89–96.
5. Nothdurft FP, Pospiech PR. Zirconium dioxide implant abutments for posterior single-tooth replacement: First results. *J Periodontol*. 2009;80:2065–2072.
6. Depprich R, Zipprich H, Ommerborn M, et al. Osseointegration of zirconia implants: An SEM observation of the bone-implant interface. *Head Face Med*. 2008;4:25.
7. Dion I, Bordenave L, Lefebvre F, et al. Physico-chemistry and cytotoxicity of ceramics. *J Mater Sci Mater Med*. 1994;5:18–24.
8. Harrnand MF. Human cell culture and characterization of cell/biomaterial interface. *Clin Mater*. 1992;11:145–150.
9. Nothdurft FP, Fontana D, Ruppenthal S, et al. Differential behavior of fibroblasts and epithelial cells on structured implant abutment materials: A comparison of materials and surface topographies. *Clin Implant Dent Relat Res*. 2015;17:1237–1249.
10. Teng F-Y, Ko C-L, Kuo H-N, et al. A comparison of epithelial cells, fibroblasts, and osteoblasts in dental implant titanium topographies. *Bioinorg Chem Appl*. 2012;2012:687291.
11. Hormia M, Könönen M, Kivilahti J, Virtanen I. Immunolocalization of proteins specific for adhaerens junctions in human gingival epithelial cells grown on differently processed titanium surfaces. *J Periodontal Res*. 1991;26:491–497.
12. Scarano A, Piattelli A, Polimeni A, Di Iorio D, Carinci F. Bacterial adhesion on commercially pure titanium and anatase-coated titanium healing screws: An in vivo human study. *J Periodontol*. 2010;81:1466–1471.
13. Rimondini L, Cerroni L, Carrassi A, Torricelli P. Bacterial colonization of zirconia ceramic surfaces: An in vitro and in vivo study. *Int J Oral Maxillofac Implants*. 2002;17:793–798.
14. Galindo-Moreno P, León-Cano A, Monje A, Ortega-Oller I, O'Valle F, Catena A. Abutment height influences the effect of platform switching on peri-implant marginal bone loss. *Clin Oral Implants Res*. 2016;27:167–173.
15. Poortinga AT, Bos R, Busscher HJ. Charge transfer during staphylococcal adhesion to TiNOX coatings with different specific resistivity. *Biophys Chem*. 2001;91:273–279.
16. Chokaree P, Poovarodom P, Chaijareenont P, Yavirach A, Rungsiyakull P. Biomaterials and clinical applications of customized healing abutment-a narrative review. *J Funct Biomater*. 2022;13:291.
17. Stimmelmayr M, Edelhoff D, Guth JF, Erdelt K, Happe A, Beuer F. Wear at the titanium-titanium and the titanium-zirconia implant-abutment interface: A comparative in vitro study. *Dent Mater*. 2012;28:1215–1220.
18. Aramouni P, Zebouni E, Tashkandi E, Dib S, Salameh Z, Almas K. Fracture resistance and failure location of zirconium and metallic implant abutments. *J Contemp Dent Pract*. 2008;9:41–48.
19. Nothdurft FP. All-ceramic zirconium dioxide implant abutments for single-tooth replacement in the posterior region: A 5-year outcome report. *Int J Prosthodont*. 2019;32:177–181.
20. Brodbeck U. The ZiReal Post: A new ceramic implant abutment. *J Esthet Restor Dent*. 2003;15:10–23.
21. Kim JS, Raigrodski AJ, Flinn BD, Rubenstein JE, Chung KH, Mancl LA. In vitro assessment of three types of zirconia implant abutments under static load. *J Prosthet Dent*. 2013;109:255–263.
22. Guncu MB, Aktas G, Guncu GN, Anıl D, Turkyilmaz I, Antonoff LR. Clinical, technical, and radiologic outcomes of 182 implant-supported zirconia single crowns using titanium-base abutments: A retrospective study. *Int J Prosthodont*. 2022;35:553–559.
23. Silva CEP, Soares S, Machado CM, et al. Effect of CAD/CAM abutment height and cement type on the retention of zirconia crowns. *Implant Dent*. 2018;27:582–587.
24. Linkevicius T, Alkimavicius J, Linkevicius R, Gineviciute E, Linkeviciene L. Effect of ti-base abutment gingival height on maintenance of crestal bone in thick biotype patients: A randomized clinical trial with 1-year follow-up. *Int J Oral Maxillofac Implant*. 2022;37:320–327.
25. Nóvoa L, Batalla P, Caneiro L, Pico A, Liñares A, Blanco J. Influence of abutment height on maintenance of peri-implant crestal bone at bone-level implants: A 3-year follow-up study. *Int J Periodontics Restor Dent*. 2017;37:721–727.
26. Galindo-Moreno P, Fernández-Jiménez A, Avila-Ortiz G, Silvestre FJ, Hernández-Cortés P, Wang HL. Marginal bone loss around implants placed in maxillary native bone or grafted sinuses: A retrospective cohort study. *Clin Oral Implant Res*. 2014;25:378–384.
27. Vervaeke S, Dierens M, Besseler J, De, Bruyn H. The influence of initial soft tissue thickness on peri-implant bone remodeling. *Clin Implant Dent Relat Res*. 2014;16:238–247.
28. Collaert B, De, Bruyn H. Early loading of four or five Astra Tech fixtures with a fixed cross-arch restoration in the mandible. *Clin Implant Dent Relat Res*. 2002;4:133–135.
29. Galindo-Moreno P, León-Cano A, Ortega-Oller I, et al. Prosthetic abutment height is a key factor in peri-implant marginal bone loss. *J Dent Res*. 2014;93:80s–85s.
30. Anusavice KJ, Kakar K, Ferree N. Which mechanical and physical testing methods are relevant for predicting the clinical performance of ceramic-based dental prostheses? *Clin Oral Implants Res*. 2007;18:218–231.
31. Gehrke P, Johannson D, Fischer C, Stawarczyk B, Beuer F. In vitro fatigue and fracture resistance of one- and two-piece CAD/CAM zirconia implant abutments. *Int J Oral Maxillofac Implant*. 2015;30:546–554.
32. Tribst J, Dal Piva A, Borges A, Bottino M. Influence of crown and hybrid abutment ceramic materials on the stress distribution of implant-supported prosthesis. *Rev Odontol UNESP*. 2018;47:149–154.
33. Van Staden RC, Guan H, Loo YC. Application of the finite element method in dental implant research. *Comput Methods Biomech Biomed Engin*. 2006;9:257–270.
34. Geng JP, Tan KB, Liu GR. Application of finite element analysis in implant dentistry: A review of the literature. *J Prosthet Dent*. 2001;85:585–598.
35. Ming-Lun H, Chih-Ling C. Application of finite element analysis in dentistry (Ch. 2). In: David M, editor. Finite Element Analysis. IntechOpen; 2010.
36. Udomsawat C, Rungsiyakull P, Rungsiyakull C, Khongkhunthian P. Comparative study of stress characteristics in surrounding bone during insertion of dental implants of three different thread designs: A three-dimensional dynamic finite element study. *Clin Exp Dent*. 2019;5:26–37.
37. Poovarodom P, Rungsiyakull C, Suriyawanakul J, et al. Effect of implant placement depth on bone remodeling on implant-supported single zirconia abutment crown: A 3D finite element study. *J Prosthodont Res*. 2023;67:278–287.
38. Rungsiyakull C, Chen J, Rungsiyakull P, Li W, Swain M, Li Q. Bone's responses to different designs of implant-supported fixed partial dentures. *Biomech Model Mechanobiol*. 2015;14:403–411.

39. Kitagawa T, Tanimoto Y, Iida T, Murakami H. Effects of material and coefficient of friction on taper joint dental implants. *J Prosthodont Res.* 2020;64:359–367.
40. Rebeeah HA, Yilmaz B, Seidt JD, McGlumphy E, Clelland N, Brantley W. Comparison of 3D displacements of screw-retained zirconia implant crowns into implants with different internal connections with respect to screw tightening. *J Prosthet Dent.* 2018;119:132–137.
41. Sevimay M, Usumez A, Eskitascioglu G. The influence of various occlusal materials on stresses transferred to implant-supported prostheses and supporting bone: A three-dimensional finite-element study. *J Biomed Mater Res B Appl Biomater.* 2005;73:140–147.
42. Hojjatie B, Anusavice KJ. Three-dimensional finite element analysis of glass-ceramic dental crowns. *J Biomech.* 1990;23:1157–1166.
43. Toksavul S, Zor M, Toman M, Gungor MA, Nergiz I, Artunc C. Analysis of dentinal stress distribution of maxillary central incisors subjected to various post-and-core applications. *Oper Dent.* 2006;31:89–96.
44. Pierrisnard L, Hure G, Barquins M, Chappard D. Two dental implants designed for immediate loading: A finite element analysis. *Int J Oral Maxillofac Implant.* 2002;17:353–362.
45. Kohal RJ, Papavasiliou G, Kamposiora P, Tripodakis A, Strub JR. Three-dimensional computerized stress analysis of commercially pure titanium and yttrium-partially stabilized zirconia implants. *Int J Prosthodont.* 2002;15:189–194.
46. Rungsiyakull C, Li Q, Sun G, Li W, Swain MV. Surface morphology optimization for osseointegration of coated implants. *Biomaterials.* 2010;31:7196–7204.
47. Weinstein AM, Klawitter JJ, Anand SC, Schuessler R. Stress analysis of porous rooted dental implants. *J Dent Res.* 1976;55:772–777.
48. Pumnil S, Rungsiyakull P, Rungsiyakull C, Elsaka S. Effect of different customized abutment types on stress distribution in implant-supported single crown: A 3D finite element analysis. *J Prosthodont.* 2022;31:e2–e11.
49. Bross I. A Confidence interval for a percentage increase. *Biometrics.* 1954;10:245–250.
50. Loehnert S, Wriggers P. Homogenisation of microheterogeneous materials considering interfacial delemination at finite strains. *Tech Mech.* 2003;23:167–177.
51. Khisaeva ZF, Ostoja-Starzewski M. On the size of RVE in finite elasticity of random composites. *J Elast.* 2006;85:153–173.
52. Canullo L, Pesce P, Patini R, Antonacci D, Tommasato G. What are the effects of different abutment morphologies on peri-implant hard and soft tissue behavior? A systematic review and meta-analysis. *Int J Prosthodont.* 2020;33:297–306.
53. Lawn BR, Deng Y, Lloyd IK, Janal MN, Rekow ED, Thompson VP. Materials design of ceramic-based layer structures for crowns. *J Dent Res.* 2002;81:433–438.
54. Jung RE, Pjetursson BE, Glauser R, Zembic A, Zwahlen M, Lang NP. A systematic review of the 5-year survival and complication rates of implant-supported single crowns. *Clin Oral Implant Res.* 2008;19:119–130.
55. Nothdurft FP, Doppler KE, Erdelt KJ, Knauber AW, Pospiech PR. Fracture behavior of straight or angulated zirconia implant abutments supporting anterior single crowns. *Clin Oral Investig.* 2011;15:157–163.
56. Gehrke P, Dhom G, Brunner J, Wolf D, Degidi M, Piattelli A. Zirconium implant abutments: Fracture strength and influence of cyclic loading on retaining-screw loosening. *Quintessence Int.* 2006;37:19–26.
57. Tribst JPM, Dal Piva AMO, Borges ALS, Anami LC, Kleverlaan CJ, Bottino MA. Survival probability, weibull characteristics, stress distribution, and fractographic analysis of polymer-infiltrated ceramic network restorations cemented on a chairside titanium base: An in vitro and in silico study. *Materials.* 2020;13:1879.

Corresponding author:
Dr Pimduen Rungsiyakull,
Faculty of Dentistry,
Chiang Mai University,
Chiang Mai 50000,
THAILAND.
Email: pimduen.rungsiyakull@cmu.ac.th.

Acknowledgments
The researchers would like to express their sincere gratitude for the advice of colleagues at the Mechanical Engineering Department, Faculty of Engineering, Khon Kaen University and for the Solid Work software, MATLAB software, and ANSYS software license. Pongsakorn Poovarodom gratefully acknowledges the CMU Presidential Scholarship, Chiang Mai University. This research was partially supported by Chiang Mai University and the Faculty of Dentistry, Chiang Mai University. The authors wish to thank Ajaan Richard L. Wilson for editing and certifying the grammatical integrity of the manuscript.

CRediT authorship contribution statement
Pimduen Rungsiyakull: Conceptualization, Methodology, Data Curation, Validation, Writing – review and editing, Supervision, Project administration. **Pongsakorn Poovarodom**: Software, Validation, Formal analysis, Investigation, Data Curation, Writing – original draft. **Chaiy Rungsiyakull**: Conceptualization, Software, Methodology, Resources, Data Curation, Supervision, Validation, Writing – review and editing. **Jarupol Suriyawanakul**: Conceptualization, Methodology, Resources. **Qing Li**: Supervision, Conceptualization, Methodology, Data Curation. **Keiichi Sasaki**: Supervision, Writing – review and editing. **Nobuhiro Yoda**: Data Curation, Writing – review and editing.

Crown Copyright © 2023 by the Editorial Council of *The Journal of Prosthetic Dentistry*. All rights reserved.
https://doi.org/10.1016/j.prosdent.2023.06.031

View publication stats